

Stochastic Modeling and Simulation of Diffuse Optical Tomography for Hemorrhage Detection in Infant Brains

Md Shafiul Alom Khan

Contents

1	Introduction	3
2	Stochastic Simulation of Photon Migration	5
2.1	Algorithm for Photon Migration	6
2.2	Simulation Methodology	8
2.3	Graphical Analysis	8
2.4	Summary	12
3	Generating Simulated Data	13
3.1	Methodology	13
3.2	Graphical Analysis of Simulated Data	13
3.3	Overall Implications of Photons Exit Matrices	15
4	Spatial Sensitivity Analysis	16
4.1	Source and Receiver Setup	16
4.2	Visualization and Detailed Analysis of Results	16
4.2.1	Interpretation	19
5	Conclusion	19
5.1	Implications of the DOT	21
5.2	Suggestions and Future Work	22
5.3	Overview	22
6	MATLAB Simulation Codes	24
6.1	Matlab Script for Stochastic Simulation of Photons	24
6.2	Matlab Script for Generating Simulated Data	27
6.3	Matlab Script for Spatial Sensitivity Analysis	29

1 Introduction

Diffuse Optical Tomography (DOT) is a new way to create images of the inside of tissues using near-infrared light. It helps doctors see details about what's going on inside the body without needing to cut or use harmful radiation. It's also cheaper than methods like X-rays or MRI. DOT is especially helpful for studying the brain and finding breast tumors early, where other methods might have limits or risks. DOT sends near-infrared light into the tissue. This light bounces around (scatters) and gets absorbed in different ways depending on what's in the tissue. The image illustrates the various paths that light can take when it enters a medium such as tissue, highlighting the complexity of light behavior in diffuse optical tomography (DOT). In DOT, light (input) is introduced into the tissue and can undergo multiple interactions, including:

- Specular Reflection: Light reflects off the surface without penetrating the tissue, following the law of reflection.
- Diffuse Reflectance: Light that enters the tissue but is scattered back towards the surface, emerging in various directions.
- Scattering: Light that penetrates deeper into the tissue is scattered multiple times, causing the light paths to meander and become highly unpredictable.
- Absorption: Some of the light is absorbed by the tissue, which is critical for imaging as different tissues absorb light differently based on their properties.
- Direct Transmission: Some light passes straight through the tissue without scattering.
- Diffuse Transmission: Light that is scattered many times within the tissue before eventually passing out of it.

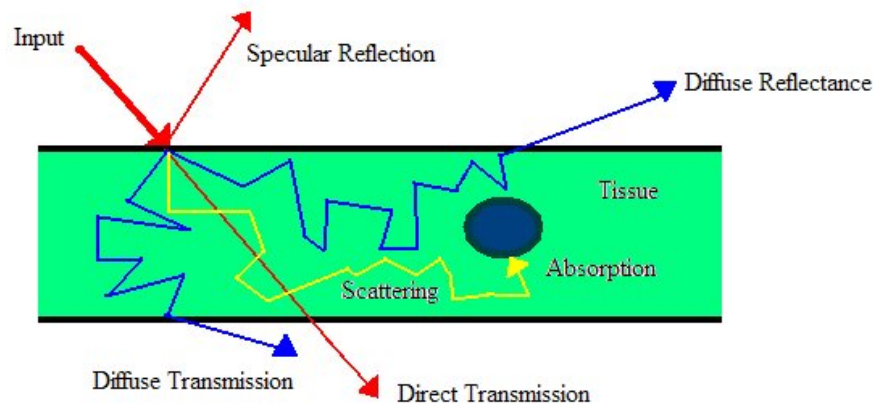


Figure 1: Light Paths Through a Tissue

In DOT, these complex light behaviors are used to reconstruct images of the tissue's internal structures. The technique relies on measuring the intensity of light that has either been transmitted through or reflected from the tissue. The detected light, which includes both absorbed

and scattered light, provides information about the tissue's optical properties. By analyzing how light is scattered and absorbed, DOT can create images that show variations in tissue properties, which may indicate physiological changes or the presence of abnormalities.

The main challenge, as depicted in the image, is that the light follows highly complicated paths due to multiple scattering events within the tissue. This scattering complicates the imaging process because it obscures the direct link between the light source and the detector, making it difficult to pinpoint where within the tissue specific interactions with light occur. DOT addresses this challenge using sophisticated mathematical models and algorithms to interpret the detected light and reconstruct an image that reflects the internal structure and function of the tissue. The behavior of this light can be calculated using a complicated math formula called the Radiative Transfer Equation (RTE). The interaction of light with the tissue components is complex and is described using the Radiative Transfer Equation (RTE). The RTE models the behavior of photons in tissue, including both absorption and scattering effects, and is given by:

$$\frac{1}{v} \frac{\partial I(\mathbf{r}, \boldsymbol{\Omega}, t)}{\partial t} + \boldsymbol{\Omega} \cdot \nabla I(\mathbf{r}, \boldsymbol{\Omega}, t) + (\mu_a(\mathbf{r}) + \mu_s(\mathbf{r})) I(\mathbf{r}, \boldsymbol{\Omega}, t) = \mu_s(\mathbf{r}) \int_{4\pi} p(\boldsymbol{\Omega}', \boldsymbol{\Omega}) I(\mathbf{r}, \boldsymbol{\Omega}', t) d\boldsymbol{\Omega}' + S(\mathbf{r}, \boldsymbol{\Omega}, t),$$

where $I(r, \Omega, t)$ is the radiance at position r in direction Ω at time t , v denotes the speed of light in the medium, while μ_a and μ_s are absorption and scattering coefficients, correspondingly, p is the phase function, and S is the source term. This formula describes how photons (light particles) move through the tissue, accounting for how they get scattered or absorbed.

Each type of tissue has unique optical properties that affect how light interacts with it. For example, hemoglobin in blood absorbs light in a special way, which allows DOT to tell the difference between healthy and unhealthy areas or measure blood oxygen levels. DOT uses simpler math by approximating the complicated RTE with a diffusion equation because light mainly scatters rather than being absorbed in most tissues. The simplified diffusion equation is:

$$-\nabla \cdot (D(\mathbf{r}) \nabla \Phi(\mathbf{r}, t)) + \mu_a(\mathbf{r}) \Phi(\mathbf{r}, t) = S(\mathbf{r}, t),$$

where $\Phi(\mathbf{r}, t)$ is related to the photon fluence rate and D is the diffusion term, defined as $\frac{1}{3\mu_a(\mathbf{r}) + \mu'_s(\mathbf{r})}$, μ'_s is the Reduced Scattering Coefficient reduced by the anisotropic factor g . This simpler equation helps predict how light spreads through the tissue and provides the data needed to create an image.

To use DOT, scientists usually solve Forward Problem(Predict how light moves through the tissue if the properties of the tissue are known) and Inverse Problem(Figure out the properties of the tissue based on the light that comes out). The inverse problem is tricky because even small errors can mess up the results. To fix this, a method called Tikhonov regularization is used in the following way:

$$\min_x \|Ax - b\|^2 + \lambda \|Lx\|^2,$$

where A represents the forward model matrix, x the unknown optical properties, b represents the measured data, λ is the regularization parameter and L is the regularization matrix.

It smooths out errors by balancing the need for accuracy with the stability of the results.

A typical DOT system involves multiple light sources and detectors that are placed around the target tissue. Advanced computational methods, such as the finite element method, iteratively solve both the forward and inverse problems, updating estimates of optical properties to match simulated and observed light distributions. In the case of brain imaging, DOT will be able to give vital information on brain activity and health by mapping blood flow and oxygenation patterns indicative of cerebral metabolism and neural activity. Correspondingly, in breast imaging, DOT’s ability to detect changes in blood volume and oxygenation provides a potent means of tumor identification that generally receives greater blood supply compared to normal tissue. It gives, in essence, the dynamic representation of how tissues work, not just mere anatomical representation, but real-time insights into physiological processes. This enables not only early detection of diseases but also significantly enhances the monitoring of disease progress and response to treatment. With continued improvements in DOT technology, driven by advances in computational techniques and optical sensors, its role in enhancing diagnostic accuracy and patient safety in healthcare is set to grow considerably. This technology gives doctors extra information about how tissues work, making it a helpful partner to traditional imaging methods—and sometimes even better.

2 Stochastic Simulation of Photon Migration

In this project, a simplified two-dimensional version of the photon migration model is used to model light propagation through a toy representation of an infant’s head. The target region is modeled as a unit circle, with a smaller circular inclusion representing a hemorrhagic lesion. This inclusion had different optical properties compared to the surrounding tissue, which allowed for the simulation of how light behaves differently in the presence of the lesion.

Photon migration can be described as a random walk process, often referred to as Levy flight. In a scattering medium, photons travel in a particular direction until they encounter a scattering or absorption event. The distance between successive scattering events is modeled as a random variable, which follows an exponential distribution characterized by a parameter, μ , known as the mean free path. The mean free path describes the average distance a photon travels before encountering an interaction.

In the Monte Carlo model used for this project, photons are initialized at a specific location along the boundary of the unit disc and propagated through the medium until they either exited the domain or are absorbed by the tissue. The photon trajectory is updated iteratively by sampling the distance to the next interaction and deciding, through a probabilistic mechanism, whether the interaction is a scattering or an absorption event.

If scattering occurred, the photon’s direction needed to be updated to reflect the scattering event. The Henyey-Greenstein distribution is used to model the scattering process, as it effectively captures the anisotropic scattering behavior of biological tissues. The Henyey-Greenstein distribution provides a probability distribution for the cosine of the scattering angle, with an anisotropy factor g that controls how strongly the light path deviates from its original direc-

tion. When $g=0$, the scattering is isotropic, while for values of g close to 1, the scattering is predominantly in the forward direction.

The optical properties of the tissue are described by the absorption coefficient (μ_a) and the scattering coefficient (μ_s) which collectively determine the likelihood of a photon being absorbed or scattered at any point. The combined coefficient ($\mu = \mu_a + \mu_s$) determines the overall interaction rate, with the mean free path being inversely proportional to μ . The relative chances of absorption and scattering are defined by the ratios $\theta_a = \mu_a/\mu$ and $\theta_b = \mu_b/\mu$ respectively. At each interaction event, a probabilistic decision is made to determine whether the photon is absorbed or scattered.

If a photon is absorbed, its trajectory ends, and it no longer contributes to the outgoing light that is measured at the tissue boundary. On the other hand, if a photon is scattered, a new direction is selected, and the photon's path continues. This process continues until the photon is either absorbed or escapes the boundary of the domain.

The Henyey-Greenstein scattering model is employed to draw new directions for scattered photons. This model provides a realistic representation of scattering in biological tissues, where photons tend to scatter in directions close to their original trajectory. The cosine of the angle between the current direction (v_c) and the new direction (v_+) is treated as a random variable distributed according to the Henyey-Greenstein function:

$$H(u | g) = \frac{1}{2} \frac{1 - g^2}{(1 - 2gu + g^2)^{3/2}}, \quad 0 \leq g < 1,$$

where g is the anisotropy factor that ranges from 0 (isotropic scattering) to 1 (highly forward-directed scattering). For each scattering event, a new scattering angle is drawn based on this distribution, ensuring that the anisotropic nature of light scattering in biological tissue is captured accurately.

2.1 Algorithm for Photon Migration

We have considered the photon migration is occurring in the homogeneous space.

Initialize:

- Current position $p_c = (x, y)$
- Initial direction $v_c = (\cos \varphi_c, \sin \varphi_c)$

Procedure:

1. Draw the Distance Traveled s :

- Photon travels a distance s before the next scattering or absorption event. s is drawn from an exponential distribution:

$$s \sim \pi(s) = \mu e^{-\mu s}$$

- Update the current position:

$$p_c \leftarrow p_c + s v_c$$

2. Decide Between Scattering or Absorption:

- Flip a coin to determine the event based on their probabilities:

$$P(\text{event} = \text{absorption}) = \theta_a, \quad P(\text{event} = \text{scattering}) = 1 - \theta_a$$

- θ_a and θ_s are the relative chances of absorption and scattering, respectively:

$$\theta_a = \frac{\mu_a}{\mu}, \quad \theta_s = \frac{\mu_s}{\mu} = 1 - \theta_a$$

3. Scattering Event: If the photon is absorbed, the simulation for this photon stops. If scattering occurs:

- Draw a sign factor $\Omega \in \{-1, +1\}$ with equal probability.
- Draw a new direction φ using the Heyney-Greenstein phase function:

$$\varphi \leftarrow \varphi_c + \Omega \arccos(u)$$

where u is calculated as:

$$u = \frac{1}{2g} \left(1 + g^2 - \left(\frac{1 - g^2}{1 + g(2\xi - 1)} \right)^2 \right), \quad \xi \sim \text{Uniform}([0, 1])$$

- Update the direction vector v_c :

$$v_c \leftarrow (\cos \varphi, \sin \varphi)$$

- Return to step 1 unless the photon exits the boundary or is absorbed.
- The entire process repeats until either the photon is absorbed or it exits the boundary of the simulated domain (e.g., the boundary of a circular region in this 2D model).
- μ is the combined scattering and absorption coefficient, μ_a is the absorption coefficient, and μ_s is the scattering coefficient. These parameters can vary within the domain if modeling different tissue types or inclusions.
- The use of the Heyney-Greenstein function ensures that the scattering angle is biased towards the forward direction, which is consistent with light behavior in scattering media like biological tissues.

This algorithm outlines the method for simulating photon migration based on the principles described in your saved study materials, focusing on the use of Monte Carlo simulations to understand the scattering and absorption processes in optical tomography.

2.2 Simulation Methodology

We write a stochastic simulator for photon migration in a two-dimensional unit circle D . The target (representing an infant's head) is modeled as a unit disc with a radius of 1, while a smaller circular inclusion Ω within the disc represented a hemorrhagic lesion. The photons are emitted from the boundary of the unit circle, and the aim is to track their movement to determine whether they are absorbed or reached the boundary. We use the Henyey-Greenstein distribution to model the new direction of each photon after scattering, which mimics the anisotropic scattering behavior of biological tissues. A relatively large anisotropy parameter value ($g = 0.8$) is used to reflect the fact that photons typically tend to scatter in directions close to their previous trajectory. Photons are stopped either if they are absorbed by the tissue or if they reached the boundary of the unit disc (∂D). If a photon reached the boundary, its point of exit is recorded. The simulation is performed with different values of the absorption coefficients μ_1 and μ_2 , which represents the absorption properties inside and outside of the inclusion Ω . The goal is to understand the difference in photon behavior when the optical properties varies between the lesion and the surrounding tissue.

2.3 Graphical Analysis

Photon Migration with Different Absorption Coefficients : In these plots, each combination of absorption coefficients μ_1 (inside the inclusion) and μ_2 (outside the inclusion) is visualized as a separate plot. Each subplot shows photon migration paths starting from the boundary, with two types of outcomes: either photons are absorbed or they escape through the boundary. Blue Paths represent the trajectories of photons that reach the boundary (∂D). These paths indicate photons that exit the domain, allowing us to determine which parts of the boundary are more likely to be reached depending on the absorption properties. Red Points denote absorption locations inside the unit circle. The more photons that get absorbed in specific areas, the stronger the color concentration in those areas. This gives insight into the spatial regions where photons are more likely to be absorbed, influenced by the difference between μ_1 and μ_2 . The variation of μ_1 and μ_2 in different plots helps illustrate how increased absorption inside the inclusion affects photon paths and exit points. For higher values of μ_1 , there is a noticeable increase in photon absorption within the lesion, resulting in fewer photons escaping through the boundary.

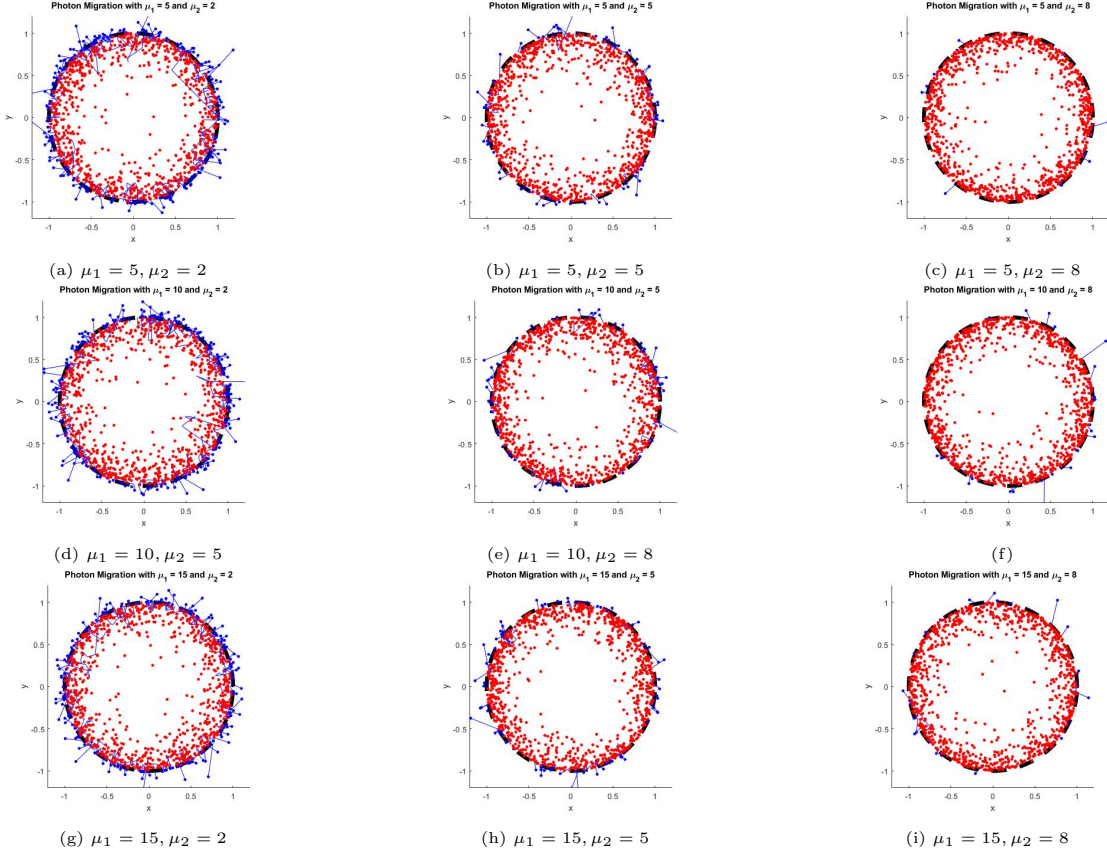


Figure 2

In the plot of Figure 2a ($\mu_1 = 5, \mu_2 = 2$), the absorption coefficient inside the lesion (μ_1) is lower compared to other cases. The red absorption points are spread across the unit circle, with a moderate concentration within the inclusion. The blue photon paths reaching the boundary indicate a relatively higher escape rate, as the absorption is not too strong inside the lesion. In the Figure 2b ($\mu_1 = 5, \mu_2 = 5$), both absorption coefficients are equal, leading to a more uniform distribution of absorbed photons throughout the unit disc. The blue escape paths are fairly evenly distributed, showing that the inclusion does not significantly alter photon behavior in this scenario. In the Figure 2c ($\mu_1 = 5, \mu_2 = 8$), with a higher absorption outside the lesion ($\mu_2 = 8$), photons are more likely to be absorbed before reaching the boundary. This results in fewer escape paths, and the red absorption points are spread more evenly but with fewer concentrated in the inclusion. In the case ($\mu_1 = 10, \mu_2 = 2$), the absorption coefficient inside the lesion ($\mu_1 = 10$) is higher, leading to a noticeable increase in the density of absorbed photons within the inclusion. The blue escape paths are fewer in number, especially near the inclusion, indicating that more photons are absorbed before reaching the boundary. When we observe for $\mu_1 = 10, \mu_2 = 5$, it is similar to the previous figure, but with a higher absorption outside the lesion, the distribution of red absorption points remains dense within the inclusion. The number of escape paths is reduced, particularly around regions close to the lesion. With both absorption coefficients being relatively high ($\mu_1 = 10, \mu_2 = 8$), the absorption points are spread evenly, with a slight concentration in the lesion. The number of escape paths is significantly lower, indicating that most photons are absorbed before reaching the boundary. In the Figure 2g ($\mu_1 = 15, \mu_2 = 2$), the high absorption inside the lesion ($\mu_1 = 15$) leads to a very dense cluster of

absorbed photons within the inclusion, and the blue escape paths are mostly located away from the lesion area. This indicates strong absorption within the lesion. The absorption remains high within the inclusion for the case $(\mu_1 = 15, \mu_2 = 5)$, with a dense cluster of red absorption points. The escape paths are fewer and mainly distributed far from the lesion. When both the inclusion and surrounding tissue have high absorption coefficients $(\mu_1 = 15, \mu_2 = 8)$, leading to a widespread distribution of absorption points with few escape paths. The photons are mostly absorbed within the disc, indicating strong absorption throughout.

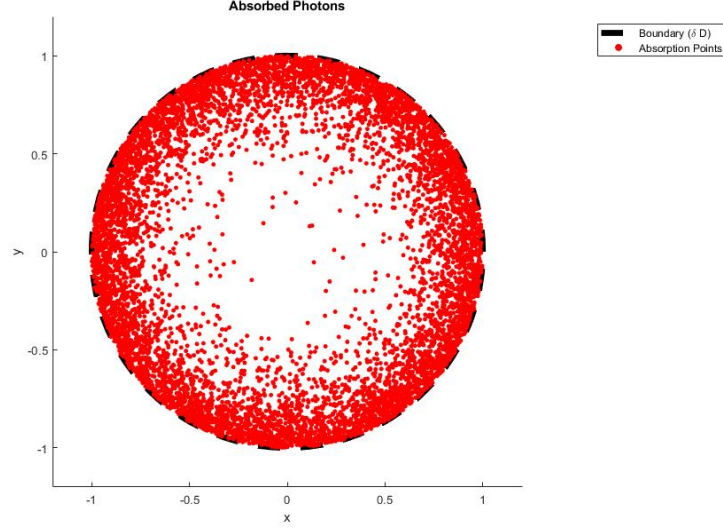


Figure 3: Distribution of Absorbed Photons

Now we observe the absorbed photons distribution figures. This figure shows the distribution of all absorbed photons across the entire unit disc D . The red scatter points illustrate where photons are absorbed during their journey, providing a visual map of absorption hot spots. The lesion (inclusion Ω) can be clearly identified as the area with higher absorption density, especially when μ_1 is larger than μ_2 . The boundary of the unit disc (∂D) is represented by the black circle, which helps visualize the spatial location of absorption within the disc. The higher concentration of red points in certain areas indicates that photons are more likely to be absorbed within the lesion. This figure allows us to understand the effect of different tissue properties on the likelihood of photon absorption. A denser cluster of points within the inclusion region (Ω) indicates that photons are more likely to be absorbed when the absorption coefficient is higher, which is consistent with biological properties of hemorrhagic lesions.

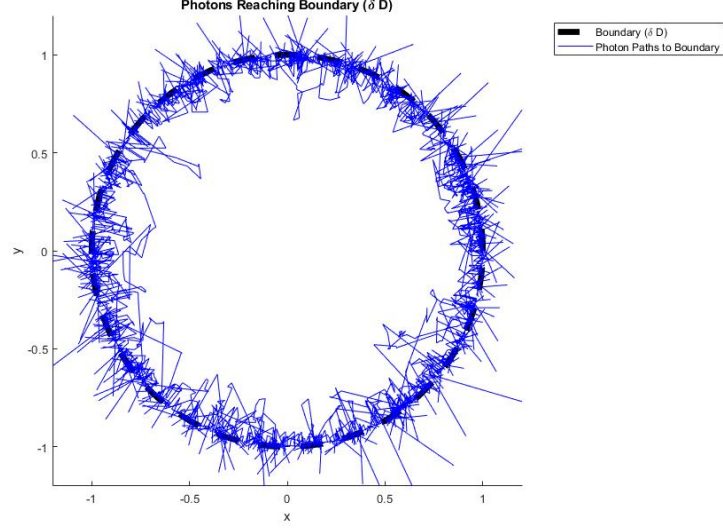


Figure 4: Photons Reaching the Boundary ∂D

We observe the motion of the photons and look what happens when they are reaching boundary (∂D). This plot shows the photon paths that reached the boundary (∂D). Each blue line represents the trajectory of a photon that escaped the domain without being absorbed. The boundary of the unit disc (∂D) is represented by the black circle, while the blue lines indicate the paths of photons that successfully escaped. By visualizing these paths, we can see which regions of the boundary are most likely to receive photons, depending on the optical properties of the inclusion and surrounding tissue. When the inclusion has a high absorption coefficient (μ_1), fewer photons escape from areas near the inclusion, leading to an uneven distribution of exit points along the boundary. This visualization provides valuable insights into how absorption properties affect photon migration and exit behavior.

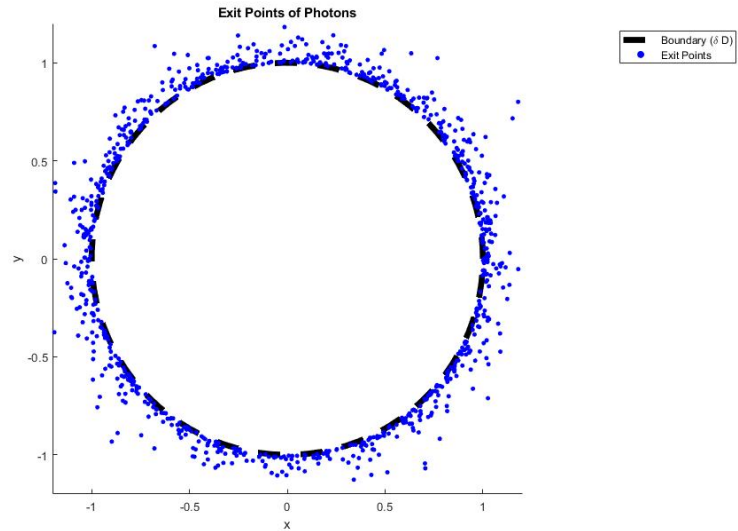


Figure 5: Exit Points of Photons

For more in depth observations of the simulation, we examine the exit points of photons. This scatter plot shows the exit points of all photons that reached the boundary. Blue points mark where photons escaped after multiple scattering events within the tissue. The boundary of the unit disc (∂D) is represented by the black circle, which helps visualize the locations where photons exited the tissue. The distribution of these points gives insight into how the inclusion (Ω) affects photon propagation. For higher values of μ_1 , there are fewer exit points near the lesion, as more photons are absorbed. This figure helps understand how the lesion modifies the overall light distribution at the tissue boundary, which is critical for reconstructing images in diffuse optical tomography (DOT).

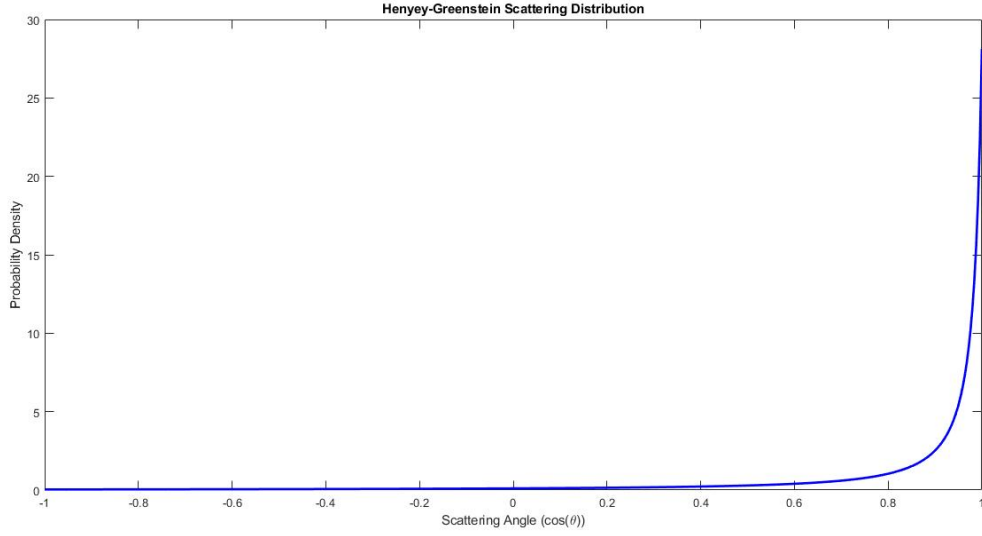


Figure 6: Henyey-Greenstein Scattering Distribution

Finally for getting an overview of the simulation we use the Henyey-Greenstein Scattering Distribution. This plot illustrates the Henyey-Greenstein scattering distribution used in the simulation. The x-axis represents the scattering angle ($\cos(\theta)$), and the y-axis represents the probability density. The parameter g controls the anisotropy of scattering. In this plot, $g = 0.8$ results in a higher probability of forward scattering, meaning that photons are more likely to continue traveling in a direction similar to their previous path. This behavior is representative of photon migration in biological tissues, where photons tend to scatter in a forward direction rather than isotropically. The distribution is highly concentrated near $\cos(\theta) = 1$, indicating a strong preference for forward scattering. This preference plays a significant role in determining photon paths and how far they travel before either being absorbed or reaching the boundary.

2.4 Summary

In short, we can say that the absorption properties of different regions (inclusion vs. surrounding tissue) significantly affect the photon migration paths, exit locations, and absorption points and higher absorption in the inclusion ($\mu_1 > \mu_2$) leads to fewer photons escaping and more being absorbed, primarily within the lesion. Again, the exit point distribution along the boundary indicates which regions are less likely to receive photons when an absorbing inclusion is present,

offering a potential method for detecting anomalies in diffuse optical tomography. Finally, the Henyey-Greenstein scattering model effectively captures the forward scattering behavior typical of photons in biological tissues, which plays a key role in how far and in what directions photons travel within the tissue.

3 Generating Simulated Data

In this section we observe the simulation to generate realistic DOT data. Let us study how an inclusion Ω would affect the light intensity measured by sensors around the boundary of the disk. The inclusion, which models a hemorrhagic lesion, is assumed to be a region with higher absorption compared to the surrounding tissue. By comparing the photon exit patterns with and without the inclusion, the simulation tried to find out whether the inclusion could be detected.

3.1 Methodology

First we have divided the unit disk into 20 equal intervals, each representing a sensor to collect photons exiting the boundary and then simulated 100,000 photons for each interval, starting from its center. Their exit locations are tracked to determine which sensor collected them. Two scenarios are analyzed :

- With Inclusion (Ω): The inclusion's absorption coefficient is $\mu_a = 15$, while the surrounding tissue has $\mu_a = 5$.
- Without Inclusion: A uniform absorption coefficient of $\mu_a = 5$ is applied across the entire disk.

The simulation results are stored in matrices showing photon exit counts for all source-sensor combinations. Heatmaps are used to visualize the photon exit distributions for both scenarios.

3.2 Graphical Analysis of Simulated Data

let's dive deeper into each of the figures and discuss their implications in greater detail. First let us observe the case where the Photon Exit Matrix With Inclusion (Ω). This matrix represents the distribution of photon exits when a hemorrhagic inclusion is present within the simulated domain (a circular disc). In DOT, this is crucial as different tissues (or inclusions) within the brain have distinct optical properties. The matrix is organized with sources along the vertical axis and sensors along the horizontal axis. Each cell in the matrix represents the count of photons that originated from a specific source position and are detected at a particular sensor position after passing through the simulated brain tissue. The color intensity in each cell shows the number of photons detected, with darker blue indicating fewer photons and yellow indicating more. The presence of the hemorrhagic inclusion likely causes higher absorption (as blood absorbs more light), leading to fewer photons reaching the sensors directly opposite the source locations near the inclusion. We can see a distinct diagonal pattern, where higher counts are seen along the diagonal from the top-left to bottom-right, suggests that photons have a higher likelihood of exiting near their source positions unless blocked or scattered by the inclusion.

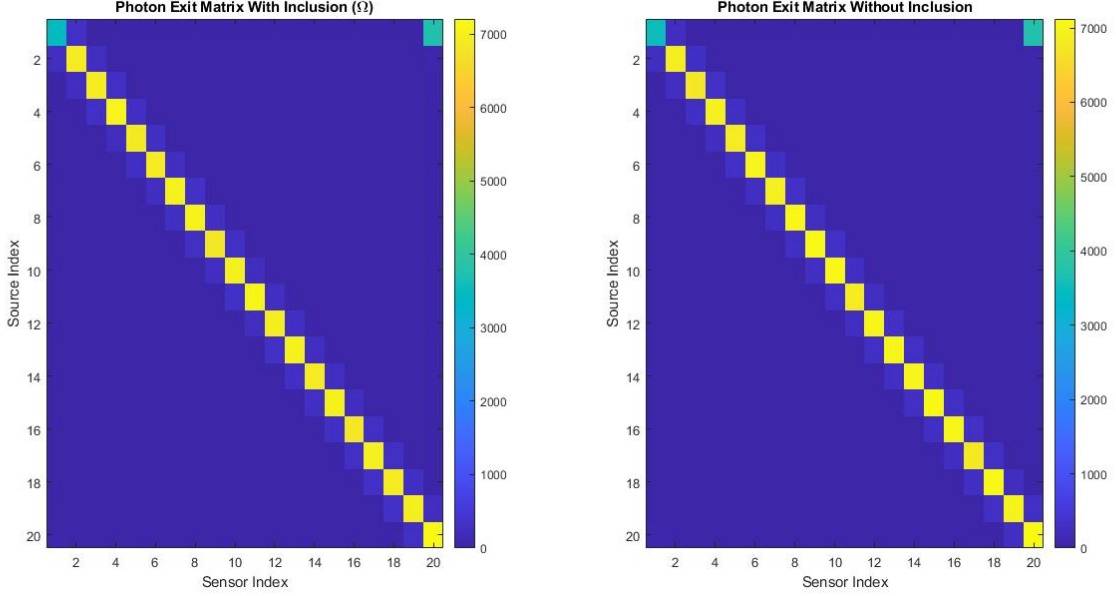


Figure 7: Comparison of Photons Exit Matrix With Ω and Without Ω

On the other hand, the matrix (Photon Exit Matrix Without Inclusion) provides a baseline or control scenario where the disc lacks the hemorrhagic inclusion, serving to understand how photons distribute in a uniform medium. Without the inclusion, the distribution of photon exits should be more uniform across the disc, as all areas within the disc have the same absorption and scattering properties. The matrix typically shows a smoother gradient of photon counts across sensors, with less variation compared to the scenario with the inclusion. The uniform properties allow photons to travel more directly from their source to the sensors without significant absorption variations, thus creating a more predictable pattern of exits across the matrix.

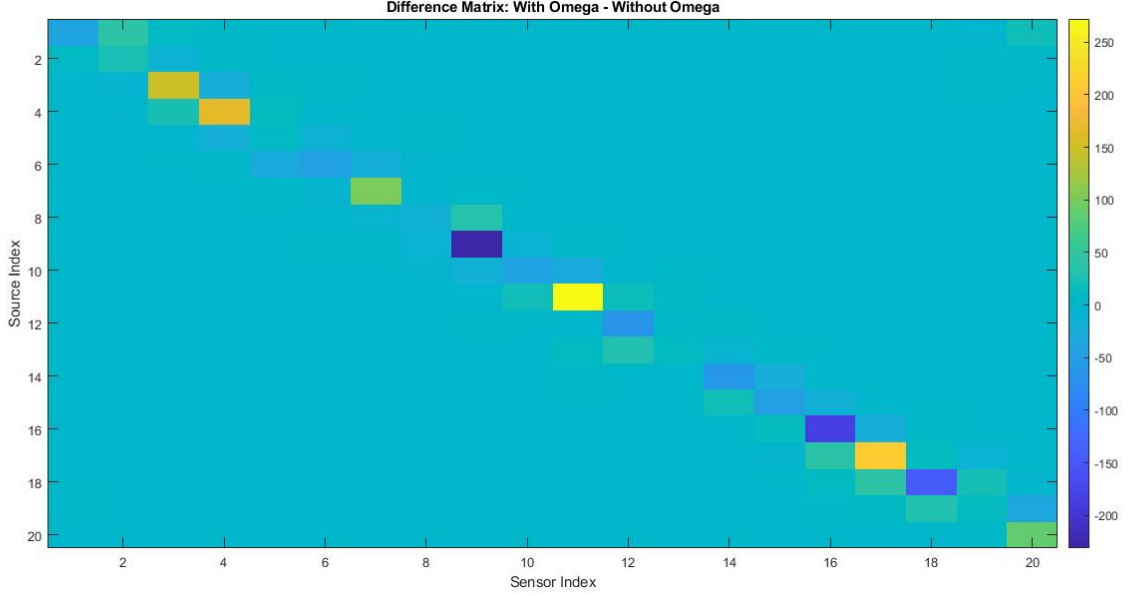


Figure 8: Difference of Photons Exit Matrix With Ω and Without Ω

To get more insights about the impacts of inclusion we observed the difference matrix. This matrix is a direct subtraction of the photon counts from the two scenarios, highlighting areas affected by the inclusion. In the figure the positive values (yellow) suggest areas where more photons are detected with the inclusion than without. This could indicate regions where photons, originally heading towards other sensors, are scattered by the inclusion towards these sensors instead. Negative values (blue) indicate fewer photons detected with the inclusion, likely due to higher absorption within the inclusion. Variations in this matrix can be analyzed to determine the sensitivity of the DOT setup. Areas with high differences (both positive and negative) are key to understanding how light interacts with the hemorrhage. This helps in fine-tuning the simulation and experimental setup for better localization and characterization of the hemorrhage.

3.3 Overall Implications of Photons Exit Matrices

Analyzing these matrices allows us to identify the most effective positions for sources and sensors to maximize information capture about the internal structure of the brain. Using the data differences, we can refine algorithms that reconstruct optical tomographic images of the brain's internal structure, aiming to improve accuracy in identifying and locating hemorrhages. In a sum, these results contribute to a deeper understanding of how light propagates through complex biological tissues, which is fundamental in enhancing DOT techniques and other optical imaging modalities. In word it can be conclude that, the matrices collectively provide a comprehensive view of the impact of internal structures on photon migration, essential for advancing DOT as a non-invasive medical imaging technology.

4 Spatial Sensitivity Analysis

We study of DOT sensitivity to changes in space: tracing the path of photons in a two-dimensional space could indicate which part of a medium contributes to the signals that are picked up by detectors. This would give a good insight into how the system responds to abnormalities, such as a hemorrhagic lesion. In this section, we have attached a laser source on the boundary of a unit disc and set a specific interval on the boundary as the receiver. Then, we trace the scattering points of photons that reached this receiver.

4.1 Source and Receiver Setup

- **Source Position** : The source is located on the boundary of the unit disc at $\mathbf{x}_s = [1, 0]$, which means photons leave from the rightmost edge of the disc and travel further inside.
- **Receiver Interval** : Along the boundary between $x_1 = 0.8$ and $x_1 = 0.9$, the receiver is placed. This portion of the boundary collects the photons leaving the medium.

The simulation followed 1,000 photons while focusing on the scattering points at which they reached the interval containing the receiver.

4.2 Visualization and Detailed Analysis of Results

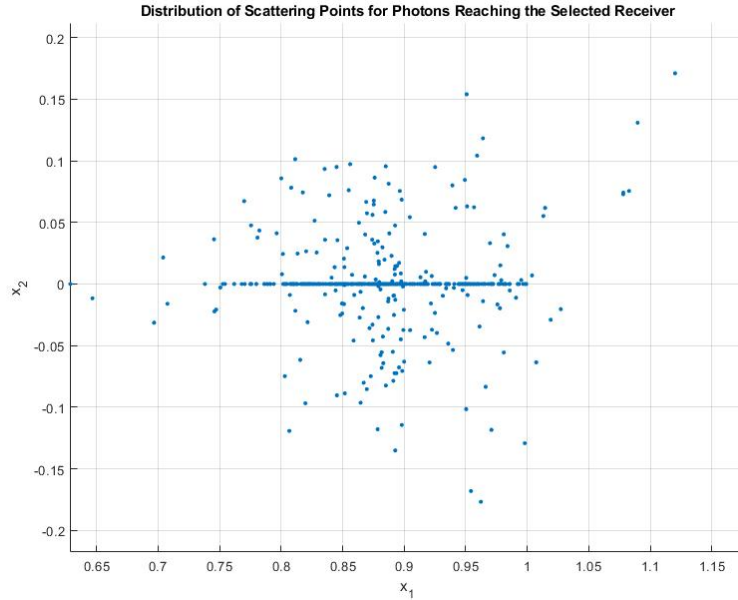


Figure 9: Distribution of Scattering Points

In Figure 9, the scatter points of photons that are received by the receiver are depicted. The horizontal axis is where the points are most densely packed within the region that encompasses the area between the source and the receiver. It would appear from this that the photons tend to scatter in regions that are close to the path that is directly from the source to the

receiver. There is a high probability that this pattern is the result of forward scattering, which is modelled according to the Heyney-Greenstein technique. In this model, photons tend to favour their initial track.

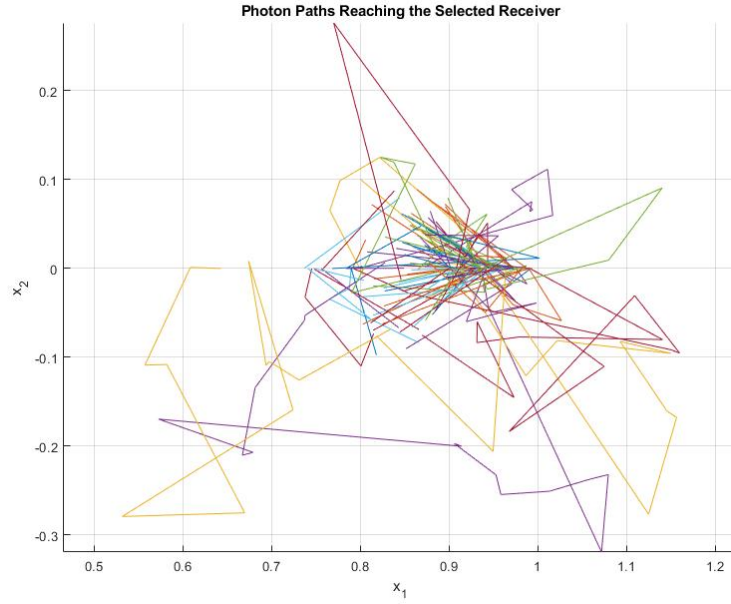


Figure 10: Photon Paths Arriving at the Selected Receiver

The path the photons took on their way to the receiver is seen in Figure 10. The paths that scattering events take are characterised by a zigzag pattern, and the trajectories are completely random. On the other hand, detected photons are frequently aligned with the direction of the source-receiver signal. Photon migration is a complicated process that requires many scattering events and some absorption before the photons reach the barrier. These routes demonstrate the complexity of photon migration.

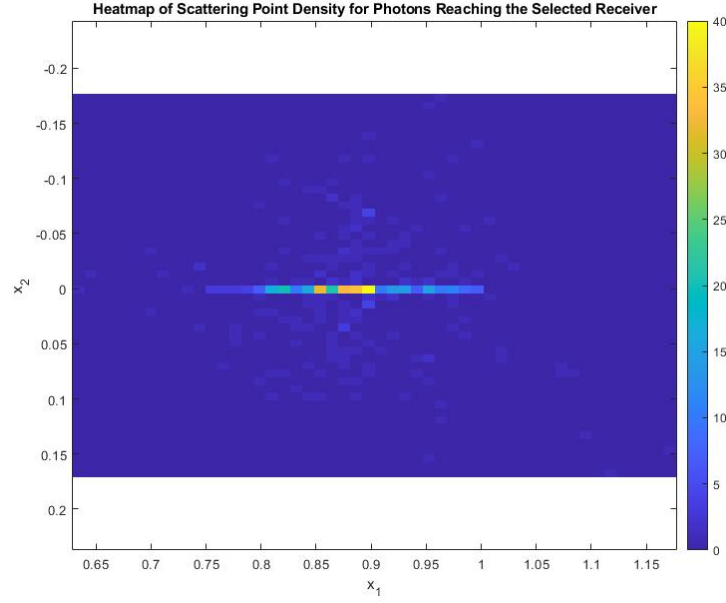


Figure 11: Heatmap of Scattering Point Density

An illustration of the heat map of the location from which photons scatter more frequently can be found in Figure 11. The majority of the scattering spots have been concentrated along the horizontal axis that runs between the source and the receiver. This highlights the fact that the routes of photons that are on their way to the receiver travel via places like these. The spatial sensitivity of certain regions is confirmed by the fact that other regions' scattering points are lower than those of other locations.

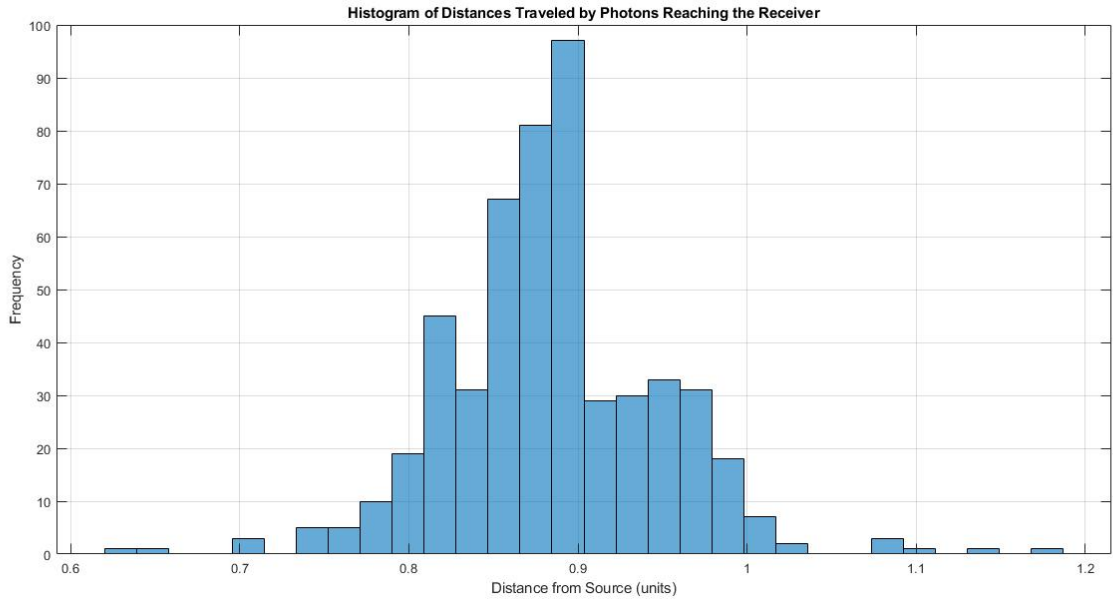


Figure 12: Histogram of Photons' Distance Traveled

The histogram which illustrates the distance that the photons have travelled in order to reach the receiver is shown in Figure 12. Both the source and the receiver are located at distances that are relatively close to the straight-line distance between them. Because of this, the majority of the signal is dominated by photons that travel along shorter paths, bringing with them a lower number of scattering events along the way. In a similar manner, the histogram displays longer lengths, which correspond to a greater number of scattered route photons that arrived at the receiver.

4.2.1 Interpretation

Analysis of scattering points, photon paths, and density visualizations describes spatial sensitivity from the DOT system. That paths and scattering points concentrate along the source-receiver direction reflects the area in space to which the system is sensitive. Large photon scattering density within that region of space contributes greatly to a detected signal.

Therefore, in such areas, if there exists an inhomogeneous inclusion such as hemorrhagic lesion, then it will significantly impact the received signal to help its detection and localization. The following analysis demonstrates how changes in optical properties—for example, due to increased absorption because of a hemorrhage—change the detected signal. Changes are more pronounced if they are located in high-density scattering regions, thereby improving detectability.

These visuals underline the spatial sensitivity of the DOT system—the paths that photons take and points at which scattering occurs, a heatmap confirms that this system is very sensitive to areas along the direct path between source and receiver. Very important in setting up sources and receivers, and for photon behavior in the medium when looking for irregularities like hemorrhagic lesions. In general, the obtained results justify the extension of studies to more complicated cases of irregularities, as well as other sensor configurations.

5 Conclusion

In this project, we have implemented a stochastic simulation of photon migration in a simplified model for diffuse optical tomography (DOT). The simulation focused on understanding how photons propagate through a medium mimicking an infant’s head with a hemorrhagic lesion. By modeling the target as a two-dimensional unit disc with an inclusion representing a lesion, this project demonstrated the influence of varying optical properties on photon migration behavior. The simulation incorporated key concepts such as absorption and scattering, represented by the coefficients μ_a and μ_s , respectively, and utilized the Henyey-Greenstein distribution to simulate photon scattering angles. This conclusion summarizes the outcomes, implications, and potential applications of the project in healthcare.

The introductory part provides a concise overview of DOT as an emerging medical imaging modality that uses near-infrared light to create functional images of biological tissues. Unlike traditional imaging methods such as X-rays or MRI, DOT is noninvasive, uses non-ionizing radiation, and is cost-effective, making it ideal for medical applications like brain imaging and

breast cancer detection. DOT is particularly useful for assessing cerebral blood flow, detecting brain hemorrhages, and monitoring hemodynamic responses.

The core of the project involved implementing a stochastic simulation to model the migration of photons through the target tissue. A unit disc is chosen as a simplified model representing an infant's head, with a smaller circular inclusion to represent a hemorrhagic lesion. The optical properties inside and outside the inclusion are characterized by different absorption coefficients (μ_1 and μ_2). The simulation followed individual photons starting from the boundary, modeled their propagation through scattering events using the Henyey-Greenstein distribution, and tracked whether they are absorbed or escaped the boundary. We observe the following:

- **Photon Absorption and Escape :** The simulation results showed how variations in the absorption coefficients (μ_1 and μ_2) affected photon behavior. For higher values of μ_1 (representing the lesion), there is an increase in photon absorption, resulting in fewer photons escaping the boundary. This behavior aligns with biological expectations since blood absorbs more light than healthy tissue.
- **Photon Paths and Exit Points :** The simulation visualized photon paths, absorption points, and exit points. The photons that are absorbed are predominantly found within the inclusion region when $\mu_1 > \mu_2$, confirming that the lesion had a significant effect on the light distribution. The photons that escaped provided information about which areas of the boundary are more likely to receive transmitted light depending on the lesion's presence.

The detailed visualizations provided a clear understanding of how light behaves in tissues with varying optical properties, contributing to our ability to detect abnormalities such as hemorrhagic lesions using DOT.

In Section 3, the unit circle is divided into equal intervals representing detectors, and photons are emitted from different source locations along the boundary. The photons that reached the boundary are recorded, and a matrix is constructed to represent the intensity distribution measured by each detector. This matrix is visualized to assess the sensitivity of the data to the inclusion. We observed:

- **Data Sensitivity to Inclusion :** By comparing simulations with and without the inclusion, it is evident that the presence of the lesion significantly affected the recorded light intensity at the detectors. The matrix representing light intensity showed differences in photon counts depending on whether the lesion is present, indicating that the data contained information about the lesion's location.
- **Practical Implications :** The results demonstrated that DOT data could potentially be used to identify the presence and position of a hemorrhage. The differences in light intensity at different detectors provided clues about the underlying tissue structure, highlighting the potential of DOT as a noninvasive diagnostic tool for detecting abnormalities.

The final section focused on understanding the spatial sensitivity of the DOT measurements. For a fixed source and selected detector, the points of scattering along photon paths that

reached the detector are saved and visualized. Our observations from the final sections are as the following:

- **Distribution of Scattering Points** : The scattering points are concentrated in regions that are most likely to affect the light detected by the selected sensor. This information is crucial for understanding which parts of the tissue contribute most to the detected signal and for improving image reconstruction algorithms by focusing on areas of high sensitivity.
- **Importance for Image Reconstruction** : The spatial sensitivity analysis helps in optimizing the placement of sources and detectors for DOT. By understanding which regions contribute most to the detected light, it is possible to design better measurement setups that maximize the sensitivity to specific tissue abnormalities, ultimately improving the accuracy of reconstructed images.

5.1 Implications of the DOT

This project has several important implications for medical healthcare, particularly in the field of noninvasive brain imaging for infants. The ability to detect hemorrhagic lesions without the use of ionizing radiation is of great value, especially for vulnerable populations such as newborns. The stochastic simulation of photon migration provides insights into how light interacts with biological tissues, which is essential for improving the accuracy and reliability of DOT as a diagnostic tool.

- **Noninvasive Detection of Hemorrhages** : The simulation demonstrated that DOT could effectively differentiate between healthy tissue and hemorrhagic lesions based on differences in light absorption. This capability is crucial for diagnosing brain hemorrhages in infants, where early detection can significantly improve outcomes. Unlike CT scans, which use ionizing radiation, DOT offers a safer alternative for repeated use, making it ideal for continuous monitoring of patients.
- **Cost-Effective and Accessible Imaging** : Compared to MRI and CT, DOT is relatively low-cost and portable. The simplicity of the equipment and the non-requirement for a controlled environment make it suitable for use in neonatal intensive care units (NICUs) and in remote areas where access to advanced medical imaging facilities is limited. The insights gained from this project could contribute to making DOT a more widely adopted technology in healthcare settings.
- **Functional Imaging Capabilities** : DOT is not only useful for structural imaging but also for functional imaging, such as monitoring cerebral oxygenation and hemodynamics. The project highlighted how photon migration is affected by different tissue properties, which could be extended to measure functional parameters like blood oxygenation levels. This is particularly useful for assessing brain function in premature infants and detecting early signs of hypoxia.
- **Optimization of Measurement Setup** : The spatial sensitivity analysis conducted in Task 4 provided valuable information for optimizing the placement of sources and detectors. By understanding which regions contribute most to the detected signal, it is possible

to improve the measurement setup, leading to higher sensitivity and better image quality. This is particularly important for clinical applications where accurate localization of abnormalities is essential for diagnosis and treatment planning.

- **Contributions to Image Reconstruction Techniques :** The simulation data generated in this project could be used to develop and validate image reconstruction algorithms for DOT. The differences in photon paths, absorption points, and exit points provide a basis for improving inverse problem-solving techniques, which are at the core of DOT image reconstruction. By incorporating probabilistic models of photon migration, it is possible to enhance the quality of reconstructed images and reduce artifacts, leading to more reliable diagnoses.

5.2 Suggestions and Future Work

While the project achieved its objectives, there are several areas where future work could further enhance the understanding and application of DOT:

- **Three-Dimensional Modeling :** Extending the simulation to three dimensions would provide a more realistic representation of photon migration in biological tissues. Although the two-dimensional model offers valuable insights, a three-dimensional model would be closer to actual clinical scenarios and could improve the accuracy of DOT simulations.
- **Incorporating More Complex Tissue Structures :** The current model assumes homogeneous tissue properties except for the inclusion. Future work could incorporate more complex tissue structures, such as multiple inclusions or layered tissues, to better represent the heterogeneity found in biological systems. This would provide a more comprehensive understanding of how different tissue types affect photon migration.
- **Real-Time Simulation and Analysis :** Developing a real-time simulation tool would be beneficial for clinical applications, allowing healthcare professionals to obtain immediate feedback on photon migration and make quicker decisions. The computational efficiency of the current stochastic model could be optimized to facilitate real-time analysis.
- **Machine Learning for Image Reconstruction :** The data generated from the photon migration simulation could be used to train machine learning models for image reconstruction. By leveraging large datasets, machine learning algorithms could learn complex patterns in photon migration and improve the accuracy and speed of DOT image reconstruction.
- **Experimental Validation :** To bridge the gap between simulation and clinical application, experimental validation using tissue phantoms or animal models is recommended. This would help verify the accuracy of the simulated results and refine the model parameters to better match experimental data.

5.3 Overview

In conclusion, this project provided a comprehensive exploration of photon migration in a simplified DOT setup, highlighting the potential of DOT as a noninvasive imaging modality for

detecting brain hemorrhages and monitoring cerebral function. The use of stochastic simulations to model photon migration offered valuable insights into the interaction between light and biological tissues, which is critical for improving DOT's diagnostic capabilities. The results demonstrated that DOT has the potential to be a safe, cost-effective, and accessible imaging tool for healthcare, particularly for vulnerable populations such as infants. Future work focusing on three-dimensional modeling, real-time analysis, and experimental validation will further enhance the applicability of DOT in clinical settings, bringing it closer to becoming a mainstream diagnostic tool in medical healthcare.

References

- [1] Calvetti, D. and Somersalo, E. (2012). Computational Mathematical Modeling - An Integrated Approach Across Scales. *Mathematical Modeling and Computation*.
- [2] Boas, D.A., Brooks, D.H., Miller, E.L., DiMarzio, C.A., Kilmer, M., Gaudette, R.J., and Zhang, Q. (2001). Imaging the body with diffuse optical tomography. *IEEE Signal Processing Magazine*, 18(6), pp.57-75.
- [3] Hoshi, Y. and Yamada, Y. (2016). Overview of diffuse optical tomography and its clinical applications. *Journal of Biomedical Optics*, 21(9), pp.091312091312.

6 MATLAB Simulation Codes

6.1 Matlab Script for Stochastic Simulation of Photons

```
1 function pht_mig
2     num_photons = 1000; % Number of photons to simulate
3     g = 0.8;           % Anisotropy factor
4     radius = 1;        % Radius of the unit disk
5     mu1_val = [5, 10, 15]; % Higher absorption in the lesion
6     mu2_val = [2, 5, 8]; % Lower absorption outside the lesion
7     all_ext_pt = [];
8     all_ab_pt = [];
9     all_b_p = {}; % Cell array for storing all photon paths reaching
10    boundary
11 % Simulate photon migration
12 for i = 1:length(mu1_val)
13     mu_1 = mu1_val(i);
14     for j = 1:length(mu2_val)
15         mu_2 = mu2_val(j);
16
17         ext_pt = [];
18         ab_pt = [];
19         b_p = {}; % Cell array to hold individual photon paths
20
21 % Run simulation for each photon
22 for photon = 1:num_photons
23     [ext_pt, photon_path, absorbed] = simulate_single_photon(
24         radius, mu_1, mu_2, g);
25     if absorbed
26         ab_pt = [ab_pt; photon_path(end, :)];
27     else
28         ext_pt = [ext_pt; ext_pt];
29         b_p{end+1} = photon_path; % Store full path if photon
30         reached the boundary
31     end
32 end
33 all_ext_pt = [all_ext_pt; ext_pt];
34 all_ab_pt = [all_ab_pt; ab_pt];
35 all_b_p = [all_b_p; b_p']; % Append using cell indexing to
36 prevent size mismatch
37
38 % Plot for current mu_1 and mu_2 combination
39 figure;
40 hold on;
41 unt_crcl(radius);
42 pth_pt(b_p, ext_pt, ab_pt);
43 title(sprintf('Photon Migration with \mu_1 = %d and \mu_2 = %d',
44     mu_1, mu_2));
45 xlabel('x');
46 ylabel('y');
47 % legend({'Boundary (\delta D)', 'Photon Paths to Boundary', '
48     Exit Points', 'Absorbed Points'}, 'Location', 'best');
49 hold off;
50 end
```



```

45     end
46     figure;
47     hold on;
48     unt_crcl(radius);
49     if ~isempty(all_ab_pt)
50         scatter(all_ab_pt(:, 1), all_ab_pt(:, 2), 15, 'r', 'filled');
51     end
52     title('Absorbed Photons');
53     xlabel('x');
54     ylabel('y');
55     legend({'Boundary (\delta D)', 'Absorption Points'}, 'Location', 'best')
56     ;
57     hold off;
58     figure;
59     hold on;
60     unt_crcl(radius);
61     for k = 1:length(all_b_p)
62         photon_path = all_b_p{k};
63         plot(photon_path(:, 1), photon_path(:, 2), 'b-');
64     end
65     title('Photons Reaching Boundary (\delta D)');
66     xlabel('x');
67     ylabel('y');
68     legend({'Boundary (\delta D)', 'Photon Paths to Boundary'}, 'Location',
69         'best');
70     hold off;
71     figure;
72     hold on;
73     unt_crcl(radius);
74     if ~isempty(all_ext_pt)
75         scatter(all_ext_pt(:, 1), all_ext_pt(:, 2), 15, 'b', 'filled');
76     end
77     title('Exit Points of Photons');
78     xlabel('x');
79     ylabel('y');
80     legend({'Boundary (\delta D)', 'Exit Points'}, 'Location', 'best');
81     hold off;
82     figure;
83     plot_hen_grn_dist(g);
84     title('Heney-Greenstein Scattering Distribution');
85     xlabel('Scattering Angle (cos(\theta))');
86     ylabel('Probability Density');
87 end
88 function [ext_pt, photon_path, absorbed] = simulate_single_photon(radius,
89     mu_1, mu_2, g)
90     theta = 2 * pi * rand(); % Random angle on the boundary
91     position = radius * [cos(theta), sin(theta)];
92     direction = -[cos(theta), sin(theta)]; % Initial direction inward
93     photon_path = position;
94     max_steps = 1000; % Set a limit to prevent infinite loops
95     for step = 1:max_steps
96         % Determine if the photon is in the lesion or outside
97         if norm(position) < 0.5 % Lesion is assumed to be a smaller circle
98             with radius 0.5
99             local_mu_a = mu_1;

```

```

96     else
97         local_mu_a = mu_2;
98     end
99     % Draw the distance traveled 's'
100    s = -log(rand()) / 10; % Exponential random variable (mean free
    path is 1/mu)
101    % Update position
102    nw_pst = position + s * direction;
103    % Add new position to path
104    photon_path = [photon_path; nw_pst];
105    % Check if the photon exits the disk
106    if norm(nw_pst) >= radius
107        ext_pt = nw_pst; % Save the exit point
108        absorbed = false;
109        return;
110    end
111    % Decide if the photon is absorbed
112    if rand() < local_mu_a / 10
113        ext_pt = [];
114        absorbed = true;
115        return;
116    end
117    direction = hen_grn(direction, g); % Scatter the photon, update
    direction using Henyey-Greenstein
118    position = nw_pst; % Update the position
119 end
120
121 % In case the photon does not exit or absorb within max_steps
122 ext_pt = [];
123 absorbed = true;
124 end
125
126 function new_direction = hen_grn(crnt_drctn, g)
127     % Draw a new direction based on the Henyey-Greenstein scattering
    function
128     xi = rand(); % Random number from uniform distribution [0,1]
129     if g == 0
130         cos_theta = 2 * xi - 1; % Uniform scattering
131     else
132         cos_theta = (1 / (2 * g)) * (1 + g^2 - ((1 - g^2) / (1 + g * (2 * xi
            - 1)))^2);
133     end
134     phi = 2 * pi * rand(); % Compute the azimuthal angle (phi) randomly in [0,
    2*pi]
135     theta = acos(cos_theta); % Convert to spherical coordinates
136
137     % Compute new direction in spherical coordinates
138     new_dx = sin(theta) * cos(phi);
139     new_dy = sin(theta) * sin(phi);
140     new_direction = [new_dx, new_dy]; % New direction as a unit vector in 2D
141 end
142
143 function unt_crcl(radius)
144     theta = linspace(0, 2 * pi, 100);
145     plot(radius * cos(theta), radius * sin(theta), 'k--', 'LineWidth', 5);

```

```

146     axis equal;
147     xlim([-1.2, 1.2]);
148     ylim([-1.2, 1.2]);
149 end
150 % Plot photon paths to the boundary, exit points, and absorption points
151 function pth_pt(b_p, ext_pt, ab_pt)
152     for k = 1:length(b_p)
153         photon_path = b_p{k};
154         plot(photon_path(:, 1), photon_path(:, 2), 'b-');
155     end
156     if ~isempty(ext_pt)
157         scatter(ext_pt(:, 1), ext_pt(:, 2), 15, 'b', 'filled');
158     end
159     if ~isempty(ab_pt)
160         scatter(ab_pt(:, 1), ab_pt(:, 2), 15, 'r', 'filled');
161     end
162 end
163 function plot_hen_grn_dist(g)
164     cos_theta = linspace(-1, 1, 500);
165     if g == 0
166         H = 1/2 * ones(size(cos_theta)); % Uniform distribution for g = 0
167     else
168         H = (1 - g^2) ./ ((1 + g^2 - 2 * g * cos_theta).^1.5) / (2 * g);
169     end
170     plot(cos_theta, H, 'b-', 'LineWidth', 2);
171 end

```

Listing 1: MATLAB code for Task 2

6.2 Matlab Script for Generating Simulated Data

```

1 function tsk3
2     % Set parameters
3     num_phtns = 1e5; % Number of photons per source position
4     m = 20; % Number of intervals (sensors)
5     g = 0.8; % Anisotropy factor
6     r = 1; % radius of the unit disk
7     % Divide the unit circle into m intervals (sensor locations)
8     theta_int = linspace(0, 2*pi, m + 1);
9     theta_int = theta_int(1:end-1); % Ignore the last point as it is the
    same as the first
10    % Prepare matrix to store photon counts for each source position
11    dm_o = zeros(m, m);
12    dm_w = zeros(m, m);
13    % Run simulation with the inclusion (Omega)
14    for source_idx = 1:m
15        source_theta = theta_int(source_idx);
16        source_pst = r * [cos(source_theta), sin(source_theta)];
17        exit_counts = simulate_photon_migration(source_pst, theta_int,
            num_phtns, r, g, true);
18        dm_o(source_idx, :) = exit_counts;
19    end
20    % Run simulation without the inclusion (Omega)
21    for source_idx = 1:m

```

```

22     source_theta = theta_int(source_idx);
23     source_pst = r * [cos(source_theta), sin(source_theta)];
24     exit_counts = simulate_photon_migration(source_pst, theta_int,
25         num_phtns, r, g, false);
26     dm_w(source_idx, :) = exit_counts;
27 end
28 % Plot the data matrix with and without Omega
29 figure;
30 subplot(1, 2, 1);
31 imagesc(dm_o);
32 colorbar;
33 title('Photon Exit Matrix With Inclusion (\Omega)');
34 xlabel('Sensor Index');
35 ylabel('Source Index');
36 subplot(1, 2, 2);
37 imagesc(dm_w);
38 colorbar;
39 title('Photon Exit Matrix Without Inclusion');
40 xlabel('Sensor Index');
41 ylabel('Source Index');
42 figure;
43 imagesc(dm_o - dm_w);
44 colorbar;
45 title('Difference Matrix: With Omega - Without Omega');
46 xlabel('Sensor Index');
47 ylabel('Source Index');
48 end
49 function exit_counts = simulate_photon_migration(source_pst, theta_int,
50     num_phtns, r, g, include_omega)
51     % Initialize exit counts for each interval
52     m = length(theta_int);
53     exit_counts = zeros(1, m);
54     % Run the simulation for each photon
55     for photon = 1:num_phtns
56         % Initialize photon direction (towards the center)
57         direction = -source_pst / norm(source_pst);
58
59         % Simulate photon migration
60         position = source_pst;
61         absorbed = false;
62         max_steps = 1000;
63
64         for step = 1:max_steps
65             % Determine if photon is in the inclusion (Omega)
66             if include_omega && norm(position) < 0.5
67                 mu_a = 15; % Absorption coefficient inside Omega
68             else
69                 mu_a = 5; % Absorption coefficient outside Omega
70             end
71             % Photon movement and possible absorption
72             s = -log(rand()) / 10; % Exponential distance with mean free
73             path of 0.1
74             nw_pst = position + s * direction;
75             % Check if photon exits the disk
76             if norm(nw_pst) >= r

```

```

74         % Determine the sensor interval for the exit point
75         exit_theta = atan2(nw_pst(2), nw_pst(1));
76         if exit_theta < 0
77             exit_theta = exit_theta + 2 * pi;
78         end
79         [~, interval_idx] = min(abs(theta_int - exit_theta));
80         exit_counts(interval_idx) = exit_counts(interval_idx) + 1;
81         break;
82     end
83     % Decide if the photon is absorbed
84     if rand() < mu_a / 10
85         absorbed = true;
86         break;
87     end
88     direction = hen_grn(direction, g);
89     position = nw_pst;
90 end
91 end
92 end
93 % Henyey-Greenstein scattering model
94 function new_direction = hen_grn(current_direction, g)
95     xi = rand(); % Random number from uniform distribution [0,1]
96     if g == 0
97         cos_theta = 2 * xi - 1; % Uniform scattering
98     else
99         cos_theta = (1 / (2 * g)) * (1 + g^2 - ((1 - g^2) / (1 + g * (2 * xi
100             - 1)))^2);
101     end
102     phi = 2 * pi * rand(); % Compute the azimuthal angle (phi) randomly in
103         [0, 2*pi]
104     theta = acos(cos_theta); % Convert to spherical coordinates
105     new_dx = sin(theta) * cos(phi);
106     new_dy = sin(theta) * sin(phi);
107     new_direction = [new_dx, new_dy]; % New direction as a unit vector in 2D
108 end

```

Listing 2: MATLAB code for Task 3

6.3 Matlab Script for Spatial Sensitivity Analysis

```

1 mu = 10; % Combined absorption and scattering coefficient
2 lambda = 1 / mu; % Mean free path
3 x0 = 0.5; % Position of the inclusion center
4 r = 0.2; % Radius of the inclusion
5 mu1 = 3; % Absorption coefficient inside inclusion
6 mu2 = 1; % Absorption coefficient outside inclusion
7 x_s = [1, 0]; % Source position on the boundary
8 rcv_int = [0.8, 0.9]; % Interval representing the receiver position
9 num_photons = 1000; % Number of photons to simulate
10 sctr_pt = []; % Arrays to store photon scattering points that reach the
    receiver
11 % Run the simulation for each photon
12 for photon_idx = 1:num_photons
13     pc = x_s;

```

```

14     vc = -x_s / norm(x_s); % Unit normal direction towards the interior
15     absorbed = false;
16     phtn_pth = [];
17     while ~absorbed
18         % Draw random step length s from exponential distribution
19         s = -log(rand) / mu;
20         pc = pc + s * vc;
21         phtn_pth = [phtn_pth; pc];
22
23         % Check if photon reaches the receiver interval
24         if pc(1) >= rcv_int(1) && pc(1) <= rcv_int(2) && abs(pc(2)) < 0.1
25             sctr_pt = [sctr_pt; phtn_pth];
26             break;
27         end
28         % Decide whether scattering or absorption occurs
29         if rand < mu1 / mu
30             absorbed = true;
31         else
32             theta = 2 * pi * rand;% Update direction
33             vc = [cos(theta), sin(theta)];
34         end
35     end
36 end
37 figure;
38 scatter(sctr_pt(:, 1), sctr_pt(:, 2), 10, 'filled');
39 xlabel('x_1');
40 ylabel('x_2');
41 title('Distribution of Scattering Points for Photons Reaching the Selected
42     Receiver');
43 axis equal;
44 grid on;
45 figure;
46 hold on;
47 for photon_idx = 1:num_photons
48     pc = x_s;
49     vc = -x_s / norm(x_s);
50     phtn_pth = [];
51     absorbed = false;
52     while ~absorbed
53         s = -log(rand) / mu;% Draw random step length s from exponential
54         distribution
55         pc = pc + s * vc;
56         phtn_pth = [phtn_pth; pc];
57         % Check if photon reaches the receiver interval
58         if pc(1) >= rcv_int(1) && pc(1) <= rcv_int(2) && abs(pc(2)) < 0.1
59             plot(phtn_pth(:, 1), phtn_pth(:, 2), '-');
60             break;
61         end
62         % Decide whether scattering or absorption occurs
63         if rand < mu1 / mu
64             absorbed = true;
65         else
66             % Update direction
67             theta = 2 * pi * rand;
68             vc = [cos(theta), sin(theta)];

```

```

67     end
68 end
69 end
70 xlabel('x_1');
71 ylabel('x_2');
72 title('Photon Paths Reaching the Selected Receiver');
73 axis equal;
74 grid on;
75 hold off;
76 figure;
77 nbins = 50;
78 [N, C] = hist3(sctr_pt, [nbins, nbins]);
79 imagesc(C{1}, C{2}, N');
80 colorbar;
81 xlabel('x_1');
82 ylabel('x_2');
83 title('Heatmap of Scattering Point Density for Photons Reaching the Selected
Receiver');
84 axis equal;
85 figure;
86 distances = sqrt(sctr_pt(:, 1).^2 + sctr_pt(:, 2).^2);
87 histogram(distances, 30);
88 xlabel('Distance from Source (units)');
89 ylabel('Frequency');
90 title('Histogram of Distances Traveled by Photons Reaching the Receiver');
91 grid on;

```

Listing 3: MATLAB code for Task 4